EUROPEAN ORGANIZATION FOR NUCLEAR RESEARCH

For internal circulation only

NP Internal Report 69-25
22 August 1969

PERFORMANCE OF LARGE CHARPAK CHAMBERS

J.H. Dieperink, K. Kleinknecht, P. Steffen and F. Vanucci

Contents

1. PURPOSE

The purpose of these tests was to select a suitable gas mixture for Charpak chambers operating as position-measuring devices[1)] and to measure detection efficiency and time resolution of those chambers with pions of ∿ 900 MeV/c using different amplifiers.

2. GEOMETRY OF CHAMBERS

The chambers were made of Vetronite frames (8 mm thick). There are four frames, two separating the grounded wire plane from the high-voltage (HV) planes, and two between the HV planes and the windows made of 120 μ Mylar. The length of the wires was 100 cm, the wire spacing 2 mm, the number of wires 300. Chamber No. 1 had gold-plated Mo-wires of 30 μ diameter and two wire meshes as HV plates. Chamber No. 2 with 20 μ Mo-Au wires had one HV plane consisting of 20 μ wires spaced at intervals of 2 mm *).

Half of the wires end on a printed board (spacing 4 mm) on one side of the chamber, the other half on the other side.

Argon was used as a counting gas and isobutane as a quenching agent.

3. MEASUREMENTS WITH SOURCE

3.1 Set-up and measurement of gas amplification

A ^{55}Fe source was used to determine the variation of the pulse height on a wire of chamber No. 1 with the high voltage applied. ^{55}Fe emits γ-rays of 5.9 keV and 3 keV, the photo peak of the 5.9 keV line gives pulse heights on the wire across a resistor of 10 M Ω (FET probe) as displayed in Fig. 1.

With the upper end of the ^{90}Sr β-spectrum, we studied the effect of different concentrations of isobutane as a quenching gas. The set-up is shown in Fig. 2. Electrons from the source are collimated in a 1 mm slit. They traverse the 120 μ Mylar window, the chamber, again a window, the thin (1 × 20 × 50 mm^3) counter and stop in the thick (10 × 120 × 120 mm^3) counter.

---

*) We thank G. Charpak for lending us chamber No. 2.

The coincidence signal (C_1C_2) of the counters is used to start the time-to-analogue converter (TAC), while the signal from the wire (through an amplifier and a trigger) stops it (Fig. 3). One wire only is used, the neighbouring wires are grounded. The output of the TAC is stored in a multichannel analyser. A typical spectrum is shown in Fig. 4 for a HV of 5.4 kV and isobutane concentration of 22%.

The jitter distribution has a peak from particles crossing the chamber near to the wire and a tail from particles passing far from the wire. If we define the peak area A to be the sum over a width of 55 nsec around the peak region, then Figs. 5a and 5b show the values of A per (C_1C_2), for two different gas mixtures. Using the values of HV at half-peak efficiency and converting them to pulse heights gives us the variation of the gas amplification with isobutane concentration (Fig. 5c). The gas amplification diminishes with increasing concentration C of isobutane, but above C = 20% there is a saturation. To be insensitive to changes in gas concentration, we chose to work at C = 25%. This means that high electric fields are needed to obtain full efficiency.

3.2 Time jitter distributions

Absolute efficiency measurements cannot be made with this arrangement because of the big scattering angles of electrons of 1 MeV. However, a comparison of amplifiers can be made if the arrangement is kept constant. Figures 6, 7 and 8 show jitter curves and peak-to-coincidence ratios [$A/(C_1C_2)$] for some amplifiers. The gas mixture differs slightly from case to case.

4. SET-UP IN BEAM

The test set-up consists of two small scintillation counters C_1 and C_2 ($7 \times 7 \times 14$ mm^3 each) in front of and behind the chamber. The counters were aligned in the beam direction such that the 14 mm long side was parallel to the wires of the chamber. Eight wires covering a width of 16 mm centred around the middle of the counters were used, each being equipped with an amplifier and a pulse shaper-stretcher.

Figure 9 shows a beam profile as defined by the coincidence (C_1C_2). The numbers plotted are the ratios of triple coincidences ($C_1C_2W_i$) per (C_1C_2), where W_i (i = 1 to 8) is the wire number i.

The electronic scheme used for the efficiency measurements is shown in Fig. 10. The overlap time between the very short (2 nsec) pulses from the wires and the (C_1C_2) coincidence output is chosen in the shaper S_W.

5. EFFICIENCY MEASUREMENTS

The efficiencies were measured for three sets of 8 amplifiers: Set A (designed by W. Sippach), Set B (designed by H. Verweij), and Set C (designed by H. Mokry). The amplifiers were not chosen selectively, so the performance should represent the average.

We show two types of graphs. In graphs of the first type the efficiency ε is plotted versus HV for a certain fixed width W. The other graphs display ε versus W for a fixed HV.

6. AMPLIFIER COMPARISON

From the curves in Figs. 11-19 and the Table it can be seen that amplifier A is the most sensitive one. The additional time jitter for the other amplifiers is due to time slewing.

With amplifier A we had problems with cross talk between the input circuitry of amplifiers on the same card; these could be removed to a level of 5% by avoiding ground loops between input and output circuitry. With the other amplifiers there were no such problems.

The probability of adjacent wire firing was measured to be 5%.

The Table gives possible operating conditions.

* * *

REFERENCE

1) G. Charpak, R. Bouclier, T. Bressani, J. Favier and Č. Zupančič, Nucl. Instrum. Meth. 62, 262 (1968).

Table 1

Possible operating conditions

Chamber	Amplifier	High voltage (kV)	ε (%)	Gate width (nsec)	Cross talk
1 (30 μ)	A	5.5 5.6 5.7	99 99.2 99.4	58 38 32	problems
1	B	5.75	98.0	70	none
1	C	5.7	98	70	none
2 (20 μ)	A	4.7 4.9 5.1 5.4	99 98 98.5 99	62 42 42 37	
2	B	5.1 5.4	98 98	60 50	none

Figure captions

Fig. 1	:	Pulse height from the ^{55}Fe 6 kV photo peak versus HV.
Fig. 2	:	Set-up for measurements with β source.
Fig. 3	:	Electronics for source measurements.
Fig. 4	:	Typical time jitter spectrum for 5.4 kV and isobutane concentration of 22%.
Fig. 5a,b	:	Counting rate A in the peak of the jitter distribution per counter coincidences (C_1C_2) as a function of HV for isobutane concentrations of 17% and 26% V1, V2, V3 are three different amplifiers.
Fig. 5c	:	Gas amplification deduced from figures (a) and (b) versus isobutane concentration. 30 μ wires.
Figs. 6,7,8	:	Time jitter spectra and HV plateaux [ratio of counting rate in peak A divided by (C_1C_2) coincidences] for different amplifiers. One wire only. V_S is the voltage at which sparking occurs. Gas a/b means that the relative volumes of argon and isobutane are a and b.
Fig. 9	:	Vertical beam profile defined by the overlap of two 7 mm large counters.
Fig. 10	:	Electronics for efficiency measurements.
Figs. 11-19	:	ε versus HV or versus W.

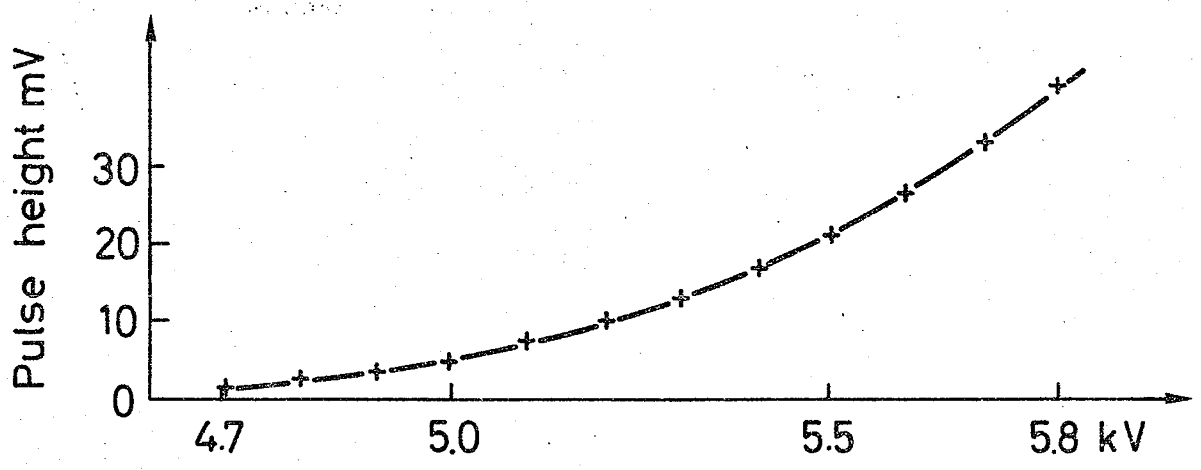
Pulse height mV
30
20
10
0
4.7
5.0
5.5
5.8 kV

FIG.1

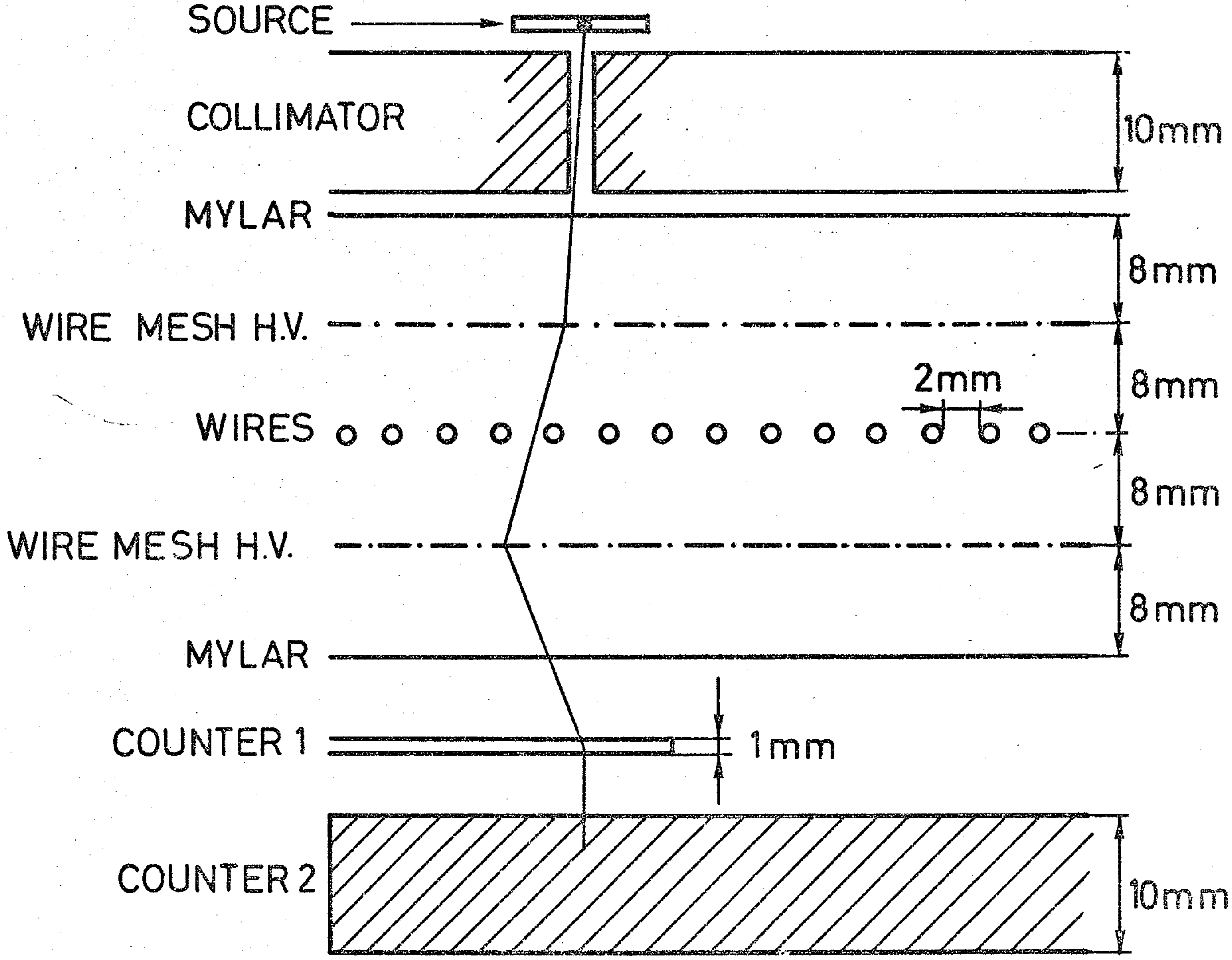
SOURCE
COLLIMATOR
MYLAR
WIRE MESH H.V.
WIRES
WIRE MESH H.V.
MYLAR
COUNTER 1
COUNTER 2
10mm
8mm
8mm
2mm
8mm
8mm
1mm
10mm

FIG.2

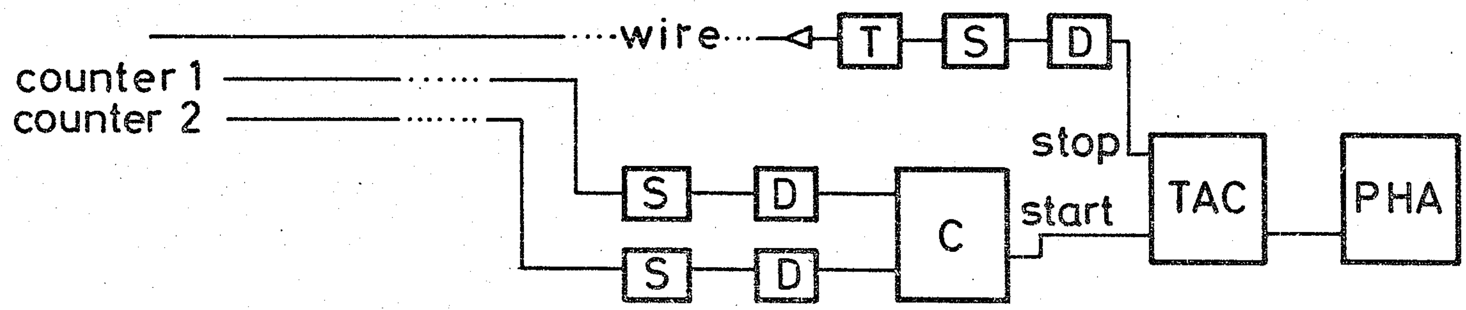

S Shaper
D Delay
T Trigger
TAC Time amplitude converter
PHA Pulse-height analyzer

FIG. 3

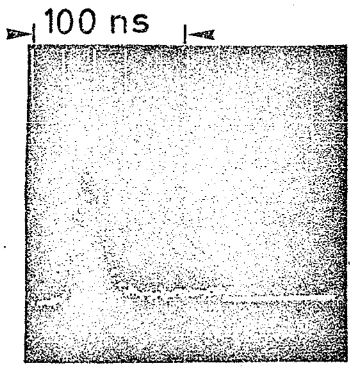

FIG. 4

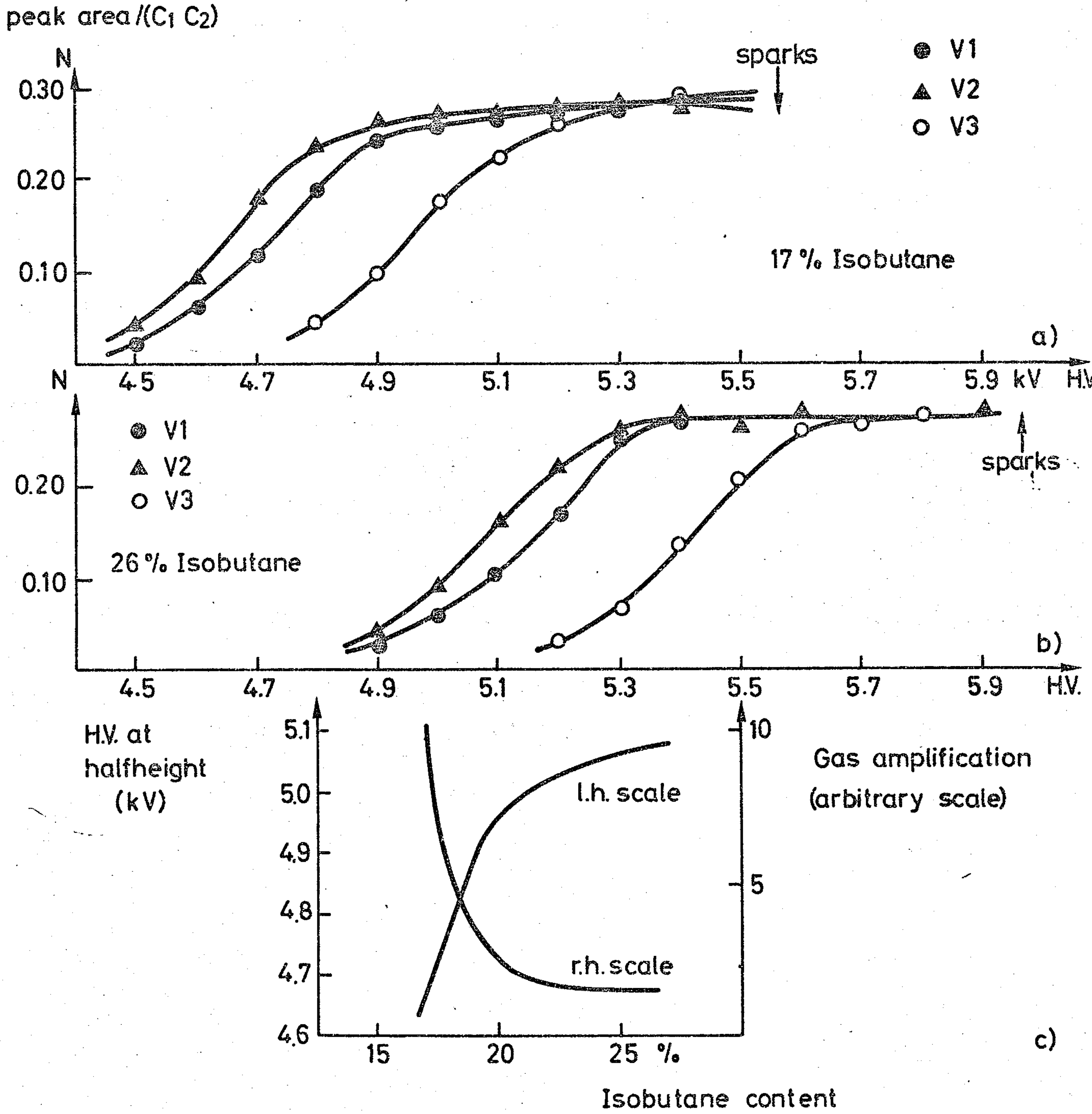
peak area /(C1 C2)
N
0.30
0.20
0.10
sparks
V1
V2
V3
17 % Isobutane
a)
4.5
4.7
4.9
5.1
5.3
5.5
5.7
5.9 kV
H.V.
N
V1
V2
V3
0.20
0.10
26 % Isobutane
sparks
b)
4.5
4.7
4.9
5.1
5.3
5.5
5.7
5.9
H.V.
H.V. at
halfheight
(kV)
5.1
5.0
4.9
4.8
4.7
4.6
15
20
25 %
l.h. scale
r.h. scale
10
5
Gas amplification
(arbitrary scale)
Isobutane content
c)

FIG.5

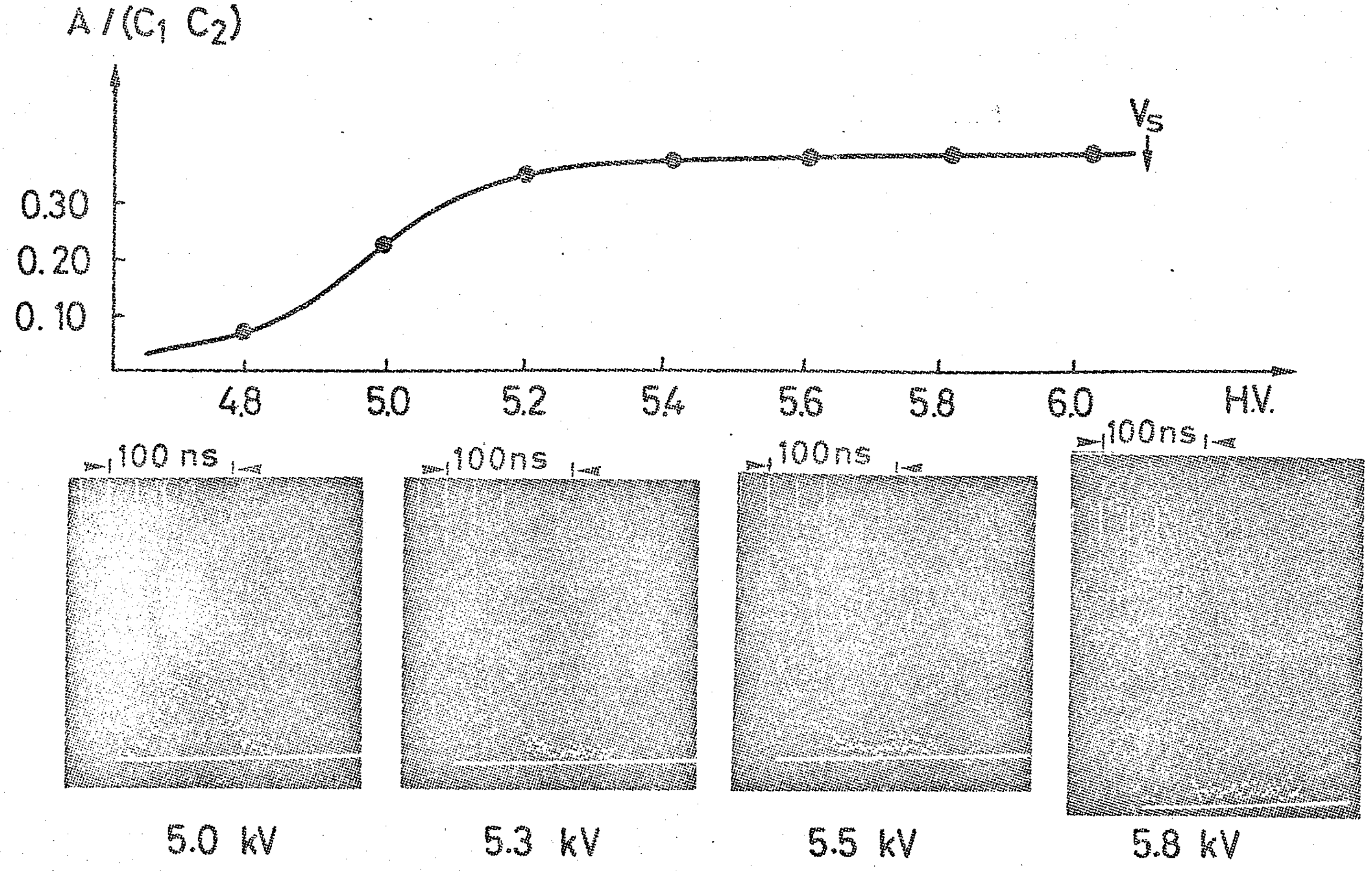

AMPLIFIER A1 (GAS 63/22) FIG.6

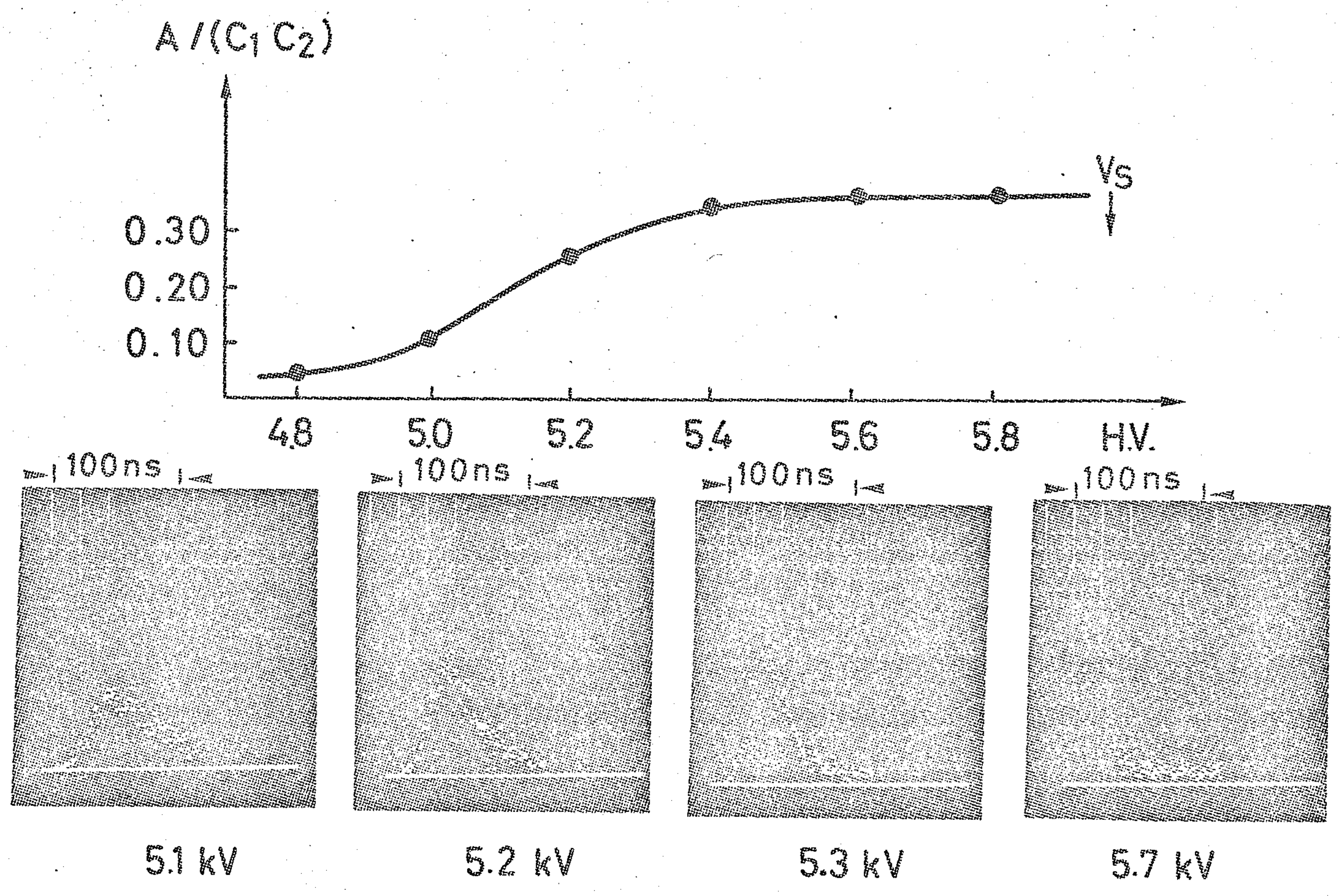

AMPLIFIER B1 (GAS 63/21) FIG.7

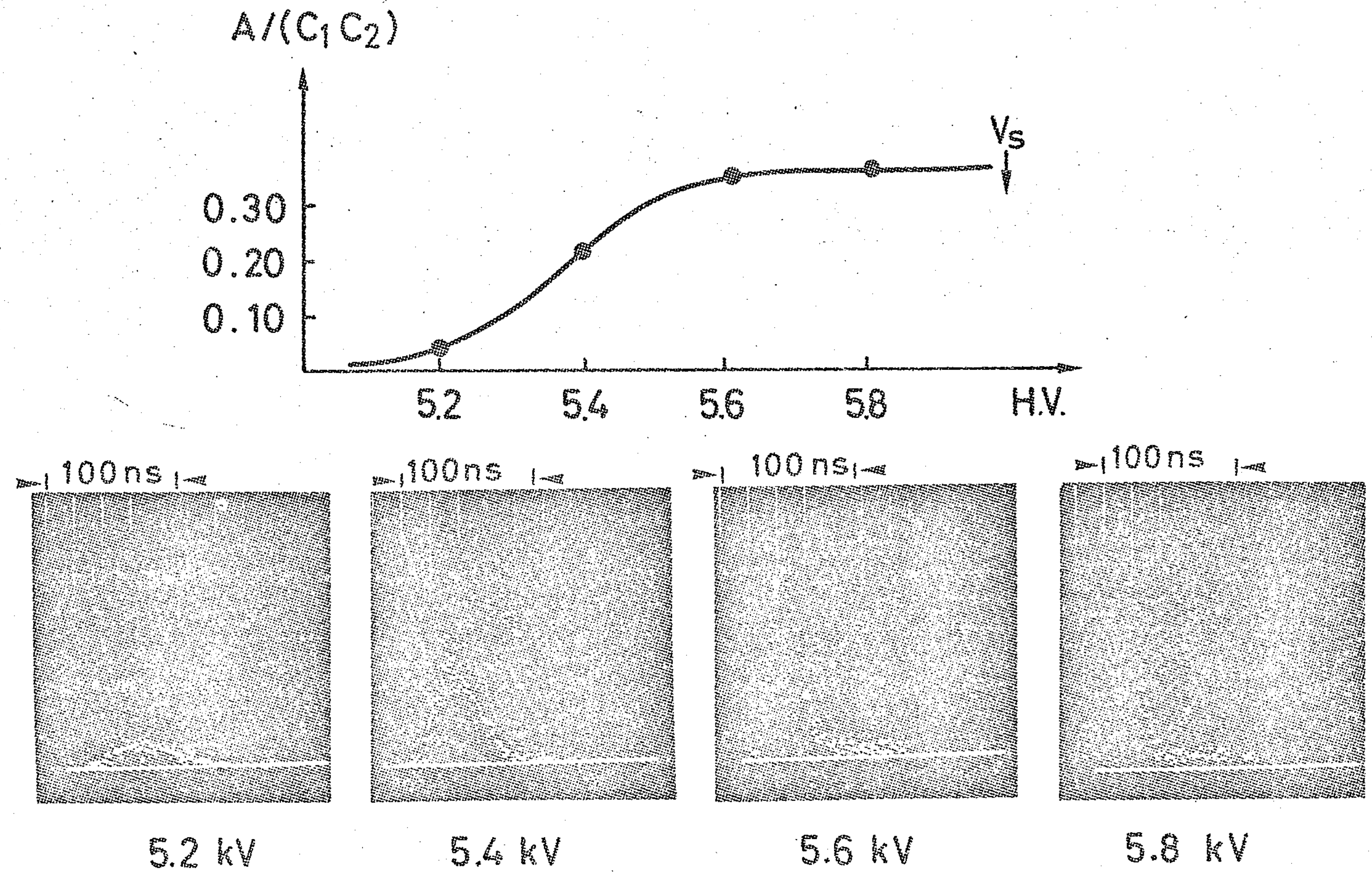

AMPLIFIER C1 (GAS 65/21) FIG. 8

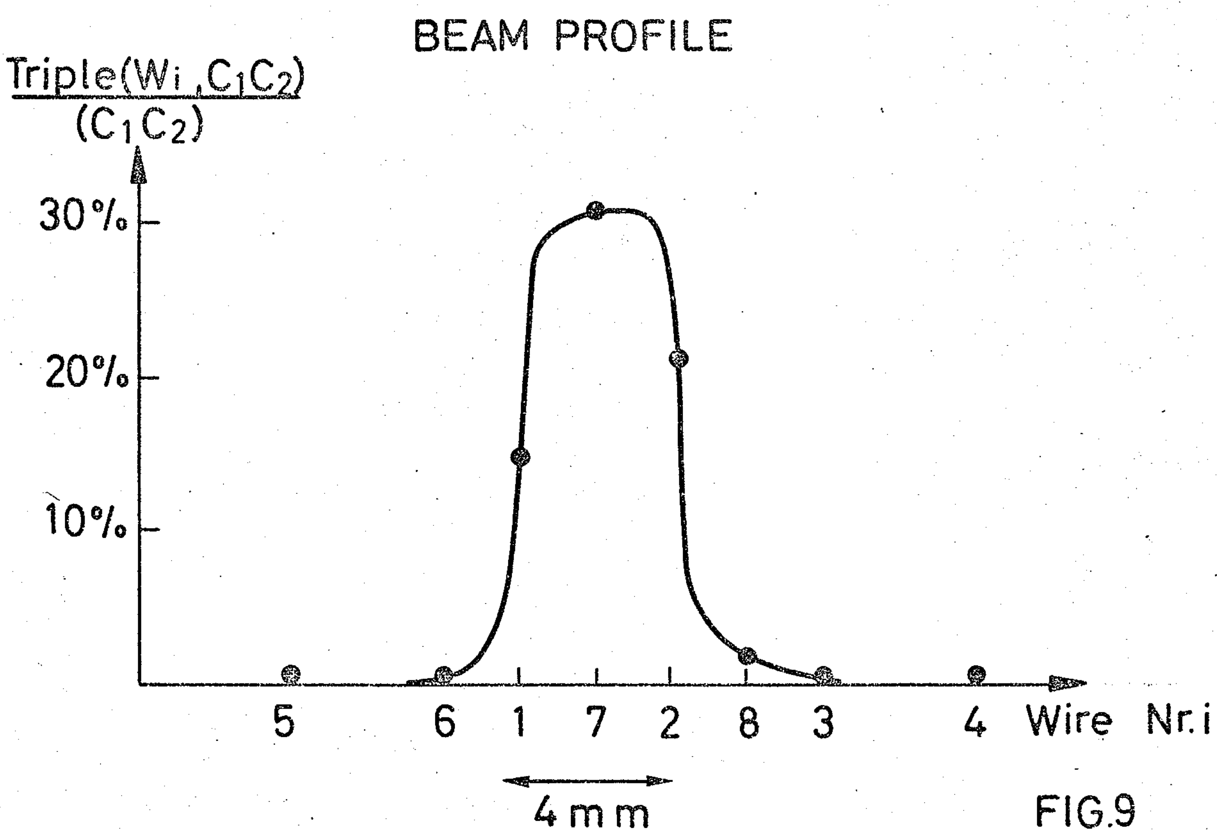
BEAM PROFILE
Triple(Wi ,C1C2) / (C1C2)
30%
20%
10%
5
6
1
7
2
8
3
4
Wire Nr.i
4mm

FIG.9

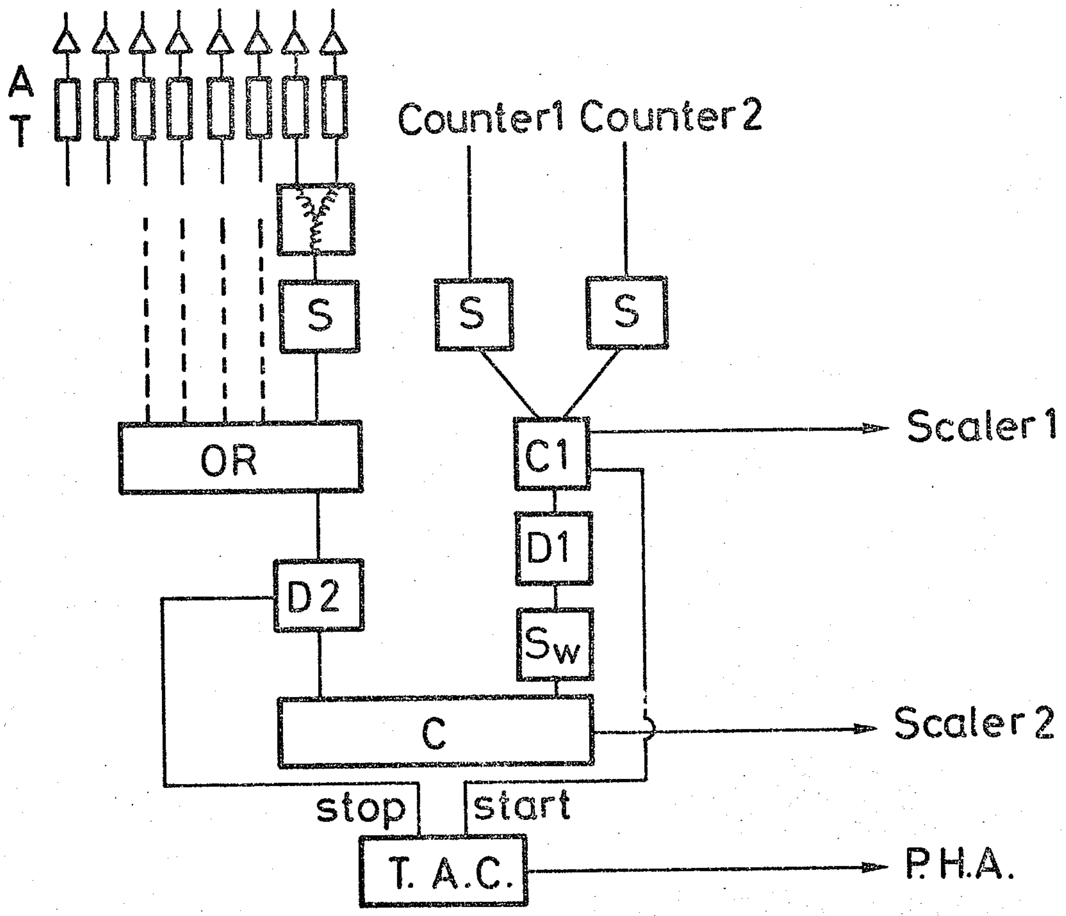

A Amplifier

T Trigger

D Delay

C Coincidence

FIG.10

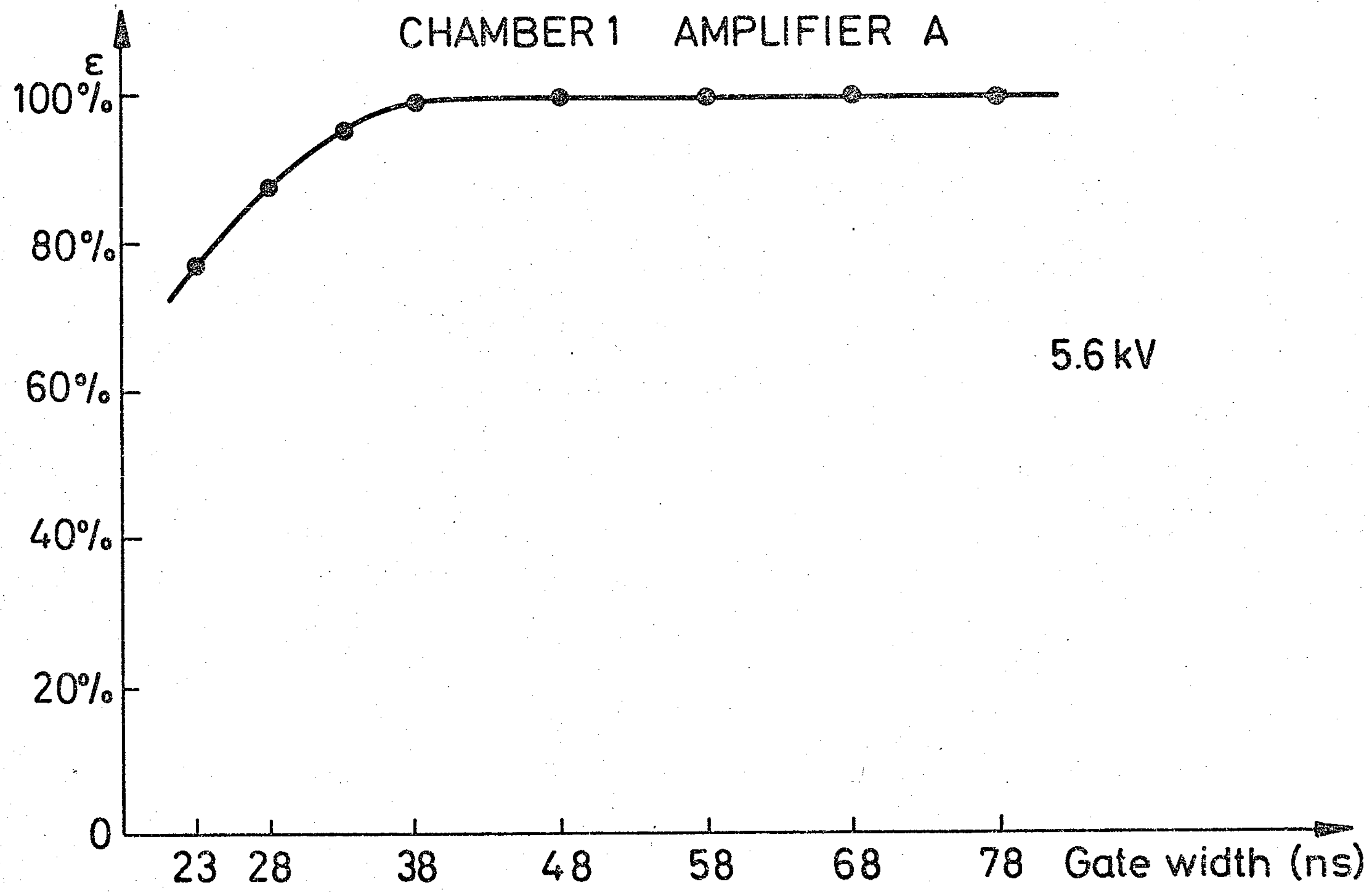

CHAMBER 1 AMPLIFIER A
ε
100%
80%
60%
40%
20%
0
5.6 kV
23
28
38
48
58
68
78
Gate width (ns)

FIG.11

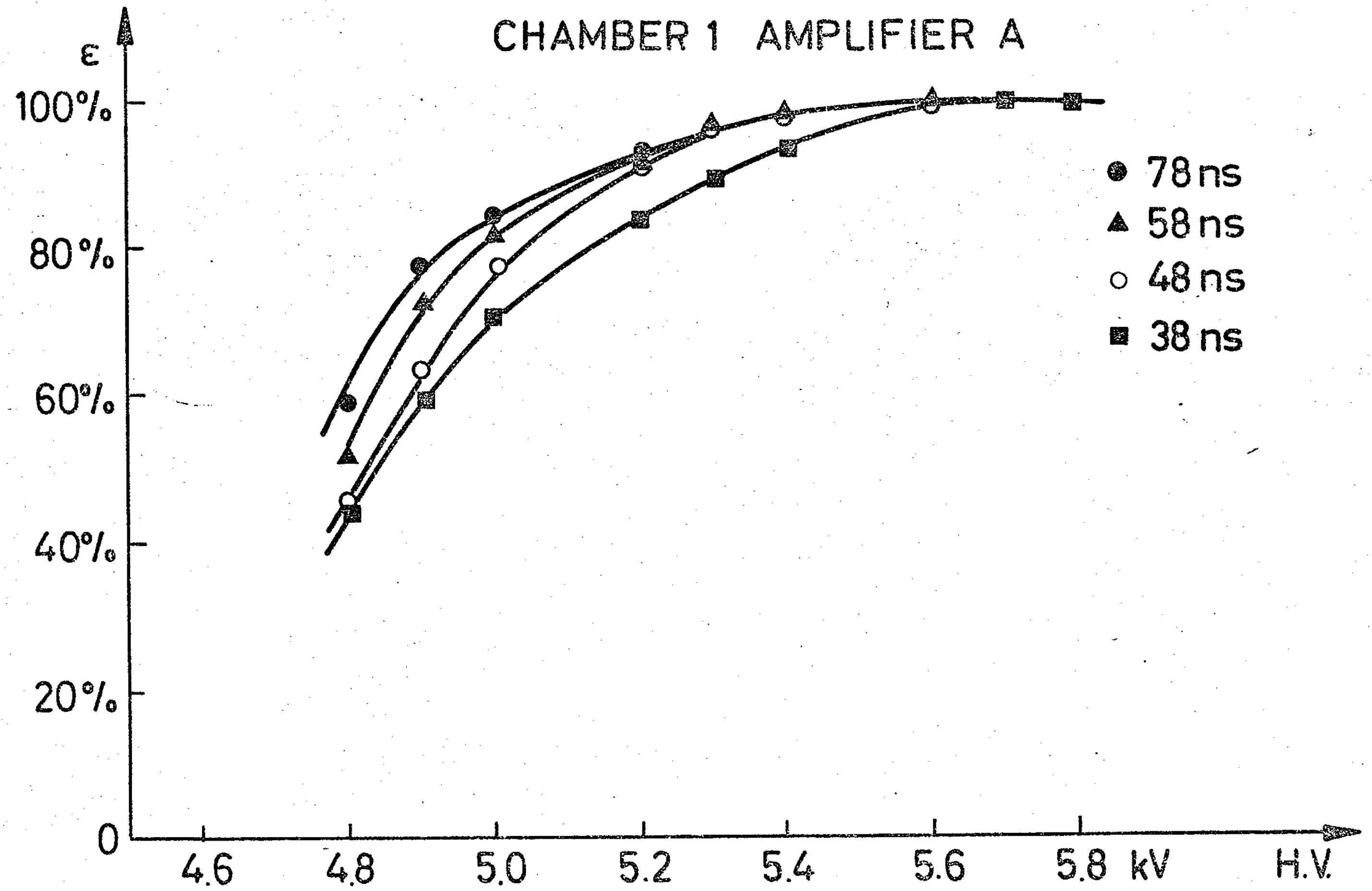

CHAMBER 1 AMPLIFIER A
ε
100%
80%
60%
40%
20%
0
78 ns
58 ns
48 ns
38 ns
4.6
4.8
5.0
5.2
5.4
5.6
5.8 kV
H.V.

FIG. 12

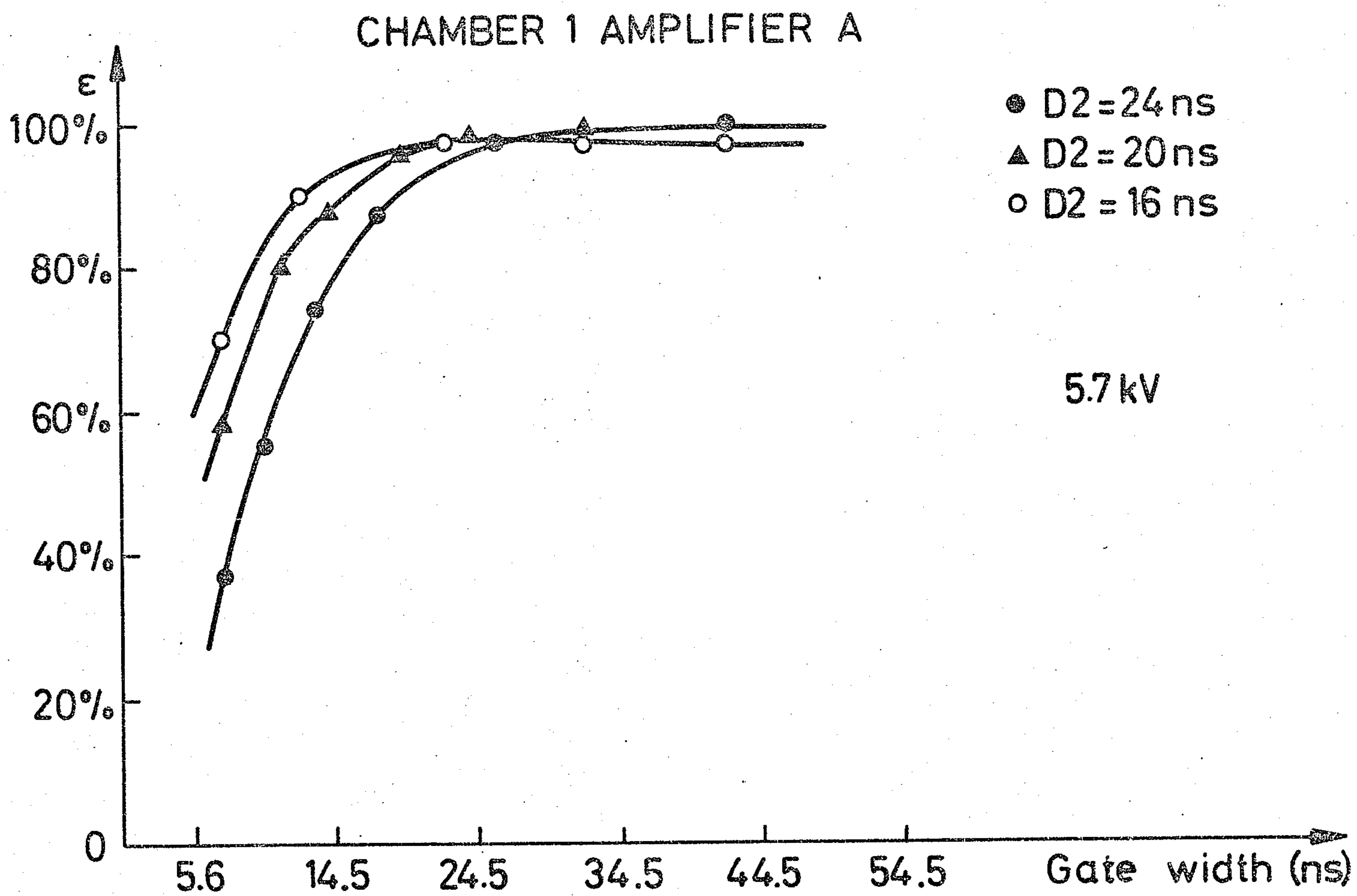
CHAMBER 1 AMPLIFIER A
ε
100%
80%
60%
40%
20%
0
D2 = 24 ns
D2 = 20 ns
D2 = 16 ns
5.7 kV
5.6
14.5
24.5
34.5
44.5
54.5
Gate width (ns)

FIG. 13

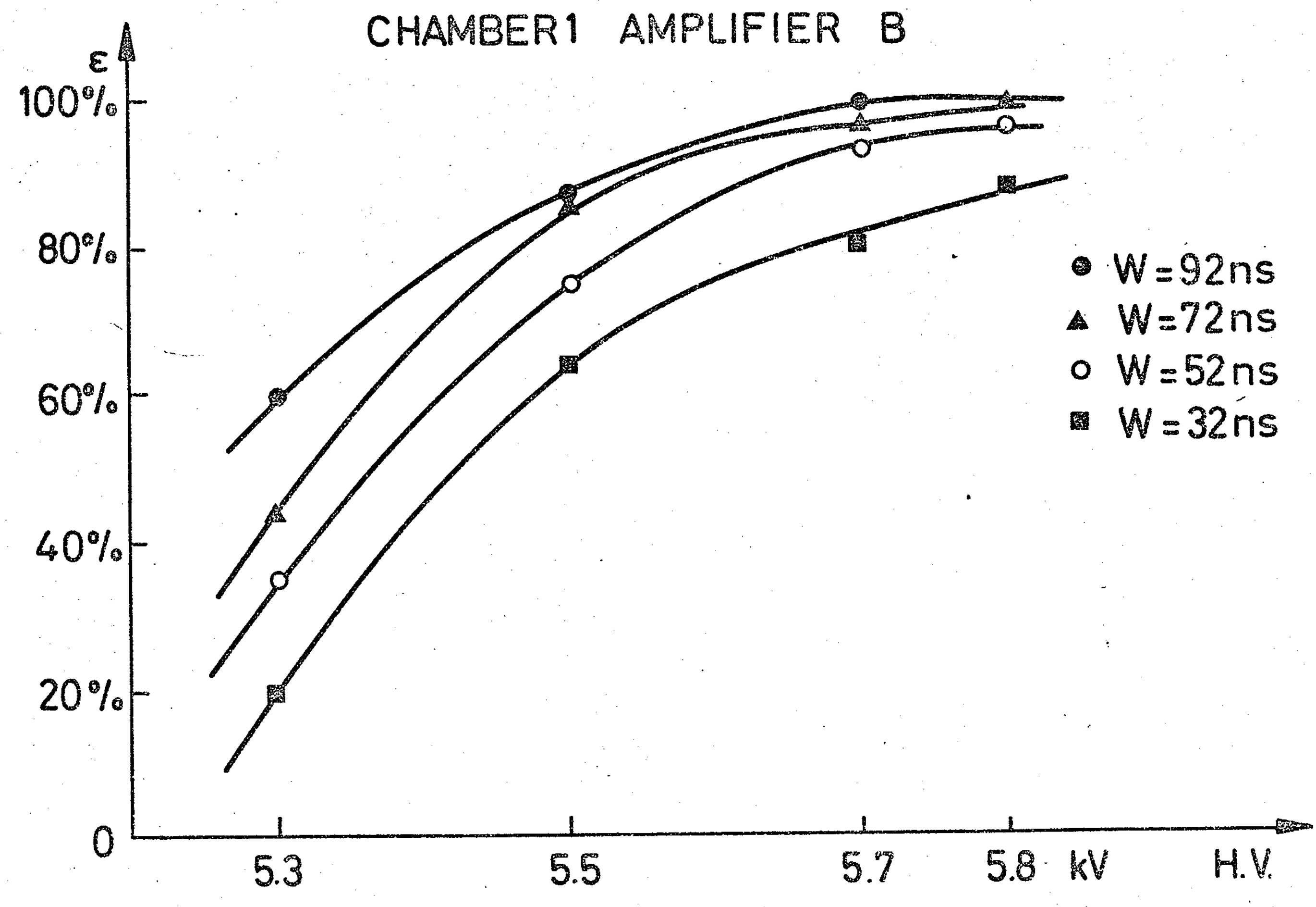
CHAMBER1 AMPLIFIER B
ε
100%
80%
60%
40%
20%
0
W = 92ns
W = 72ns
W = 52ns
W = 32ns
5.3
5.5
5.7
5.8 kV
H.V.

FIG. 14

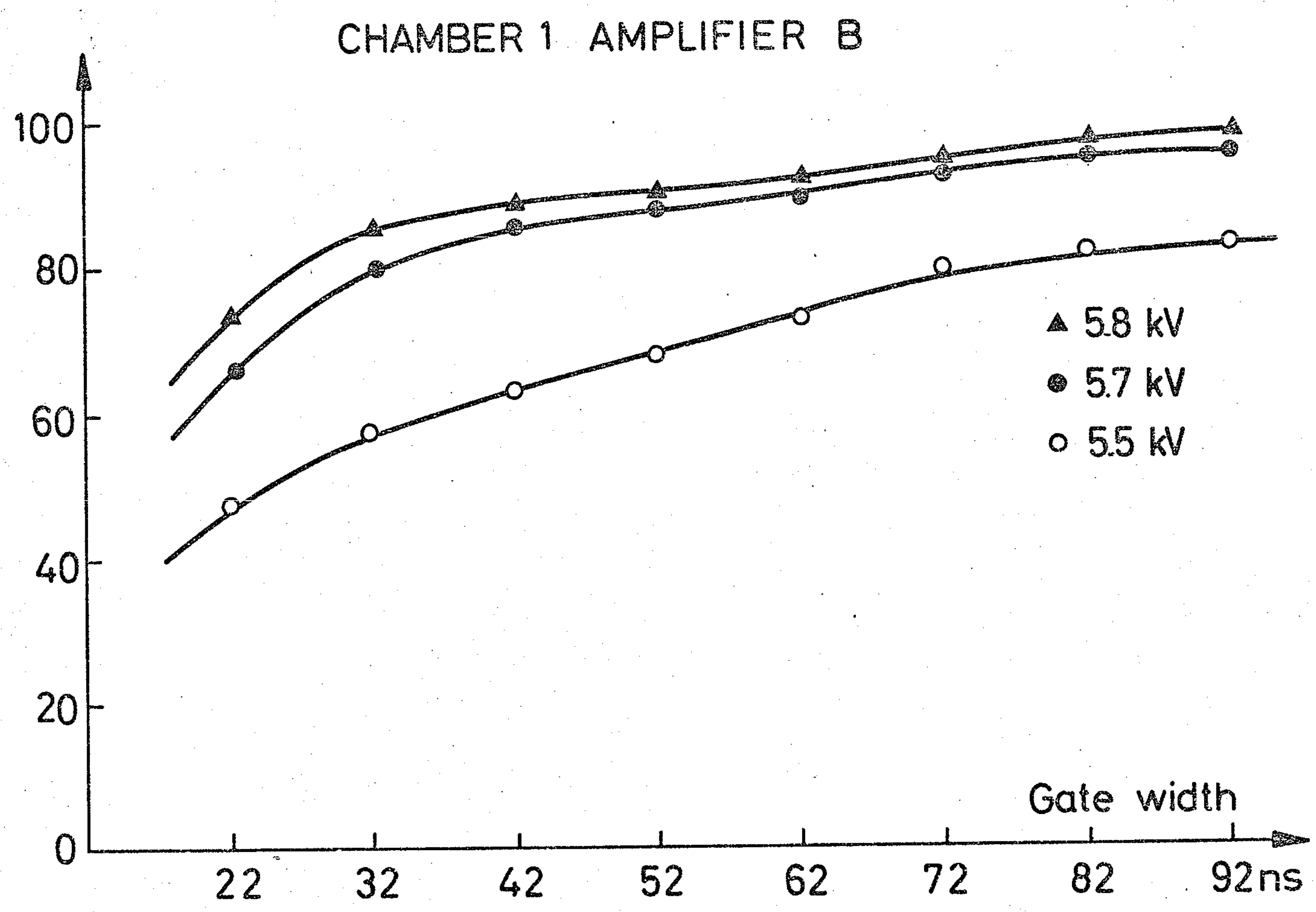
CHAMBER 1 AMPLIFIER B
100
80
60
40
20
0
▲ 5.8 kV
● 5.7 kV
○ 5.5 kV
Gate width
22
32
42
52
62
72
82
92ns
FIG. 15

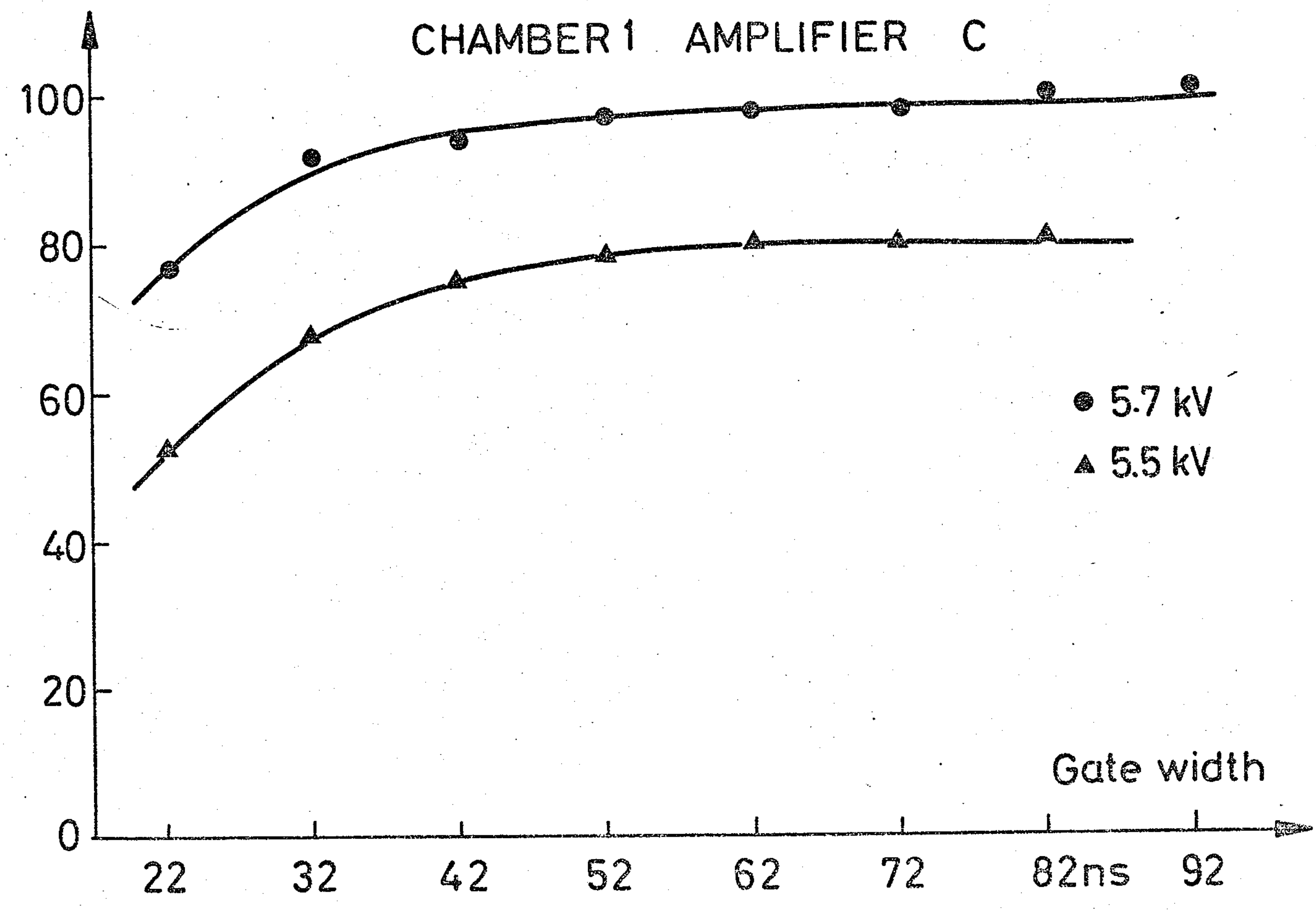
CHAMBER 1 AMPLIFIER C
100
80
60
40
20
0
● 5.7 kV
▲ 5.5 kV
Gate width
22
32
42
52
62
72
82ns
92
FIG.16

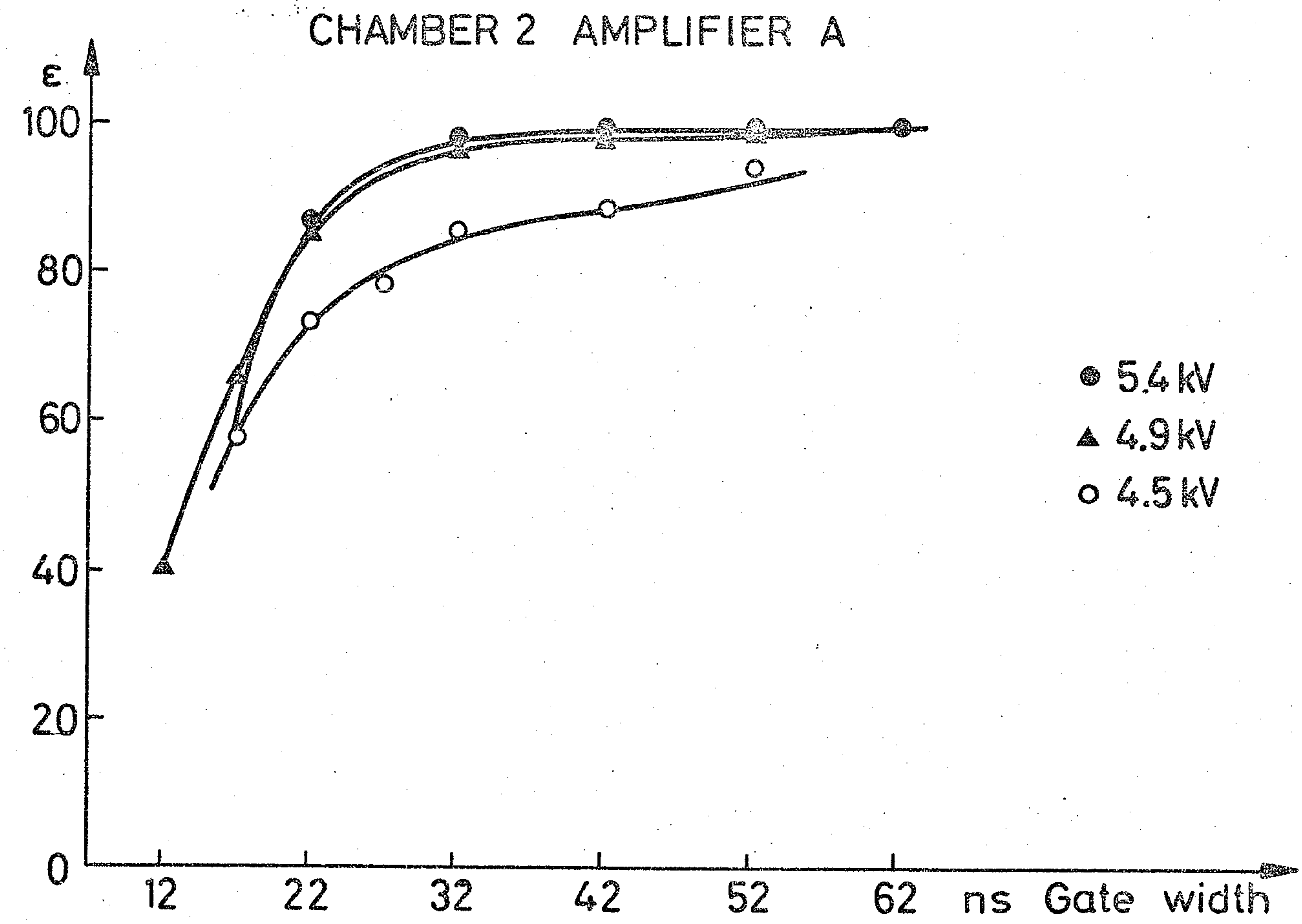

CHAMBER 2 AMPLIFIER A
ε
100
80
60
40
20
0
12
22
32
42
52
62
ns Gate width
5.4 kV
4.9 kV
4.5 kV

FIG. 17

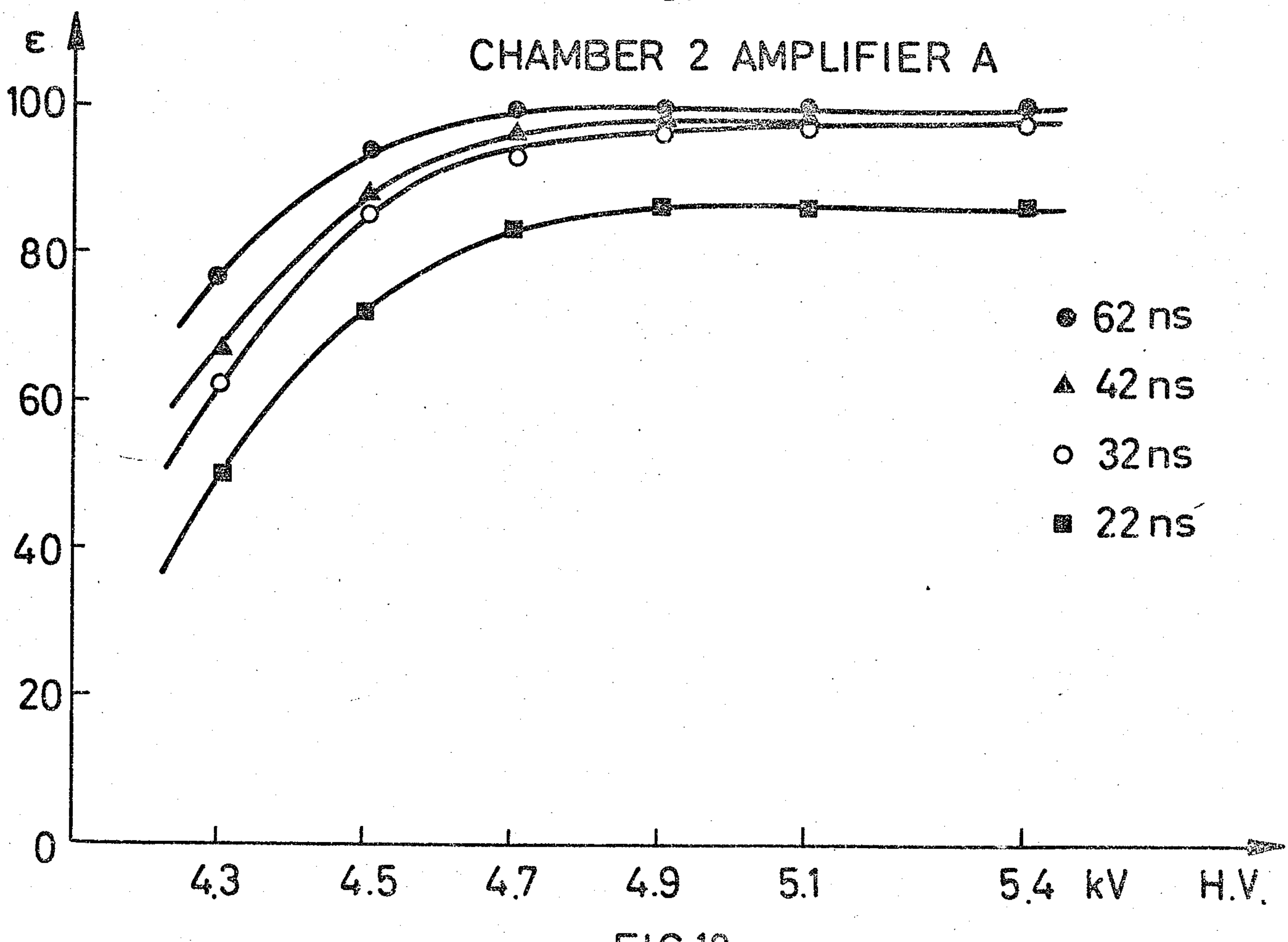

CHAMBER 2 AMPLIFIER A
ε
100
80
60
40
20
0
4.3
4.5
4.7
4.9
5.1
5.4 kV
H.V.
62 ns
42 ns
32 ns
22 ns

FIG.18

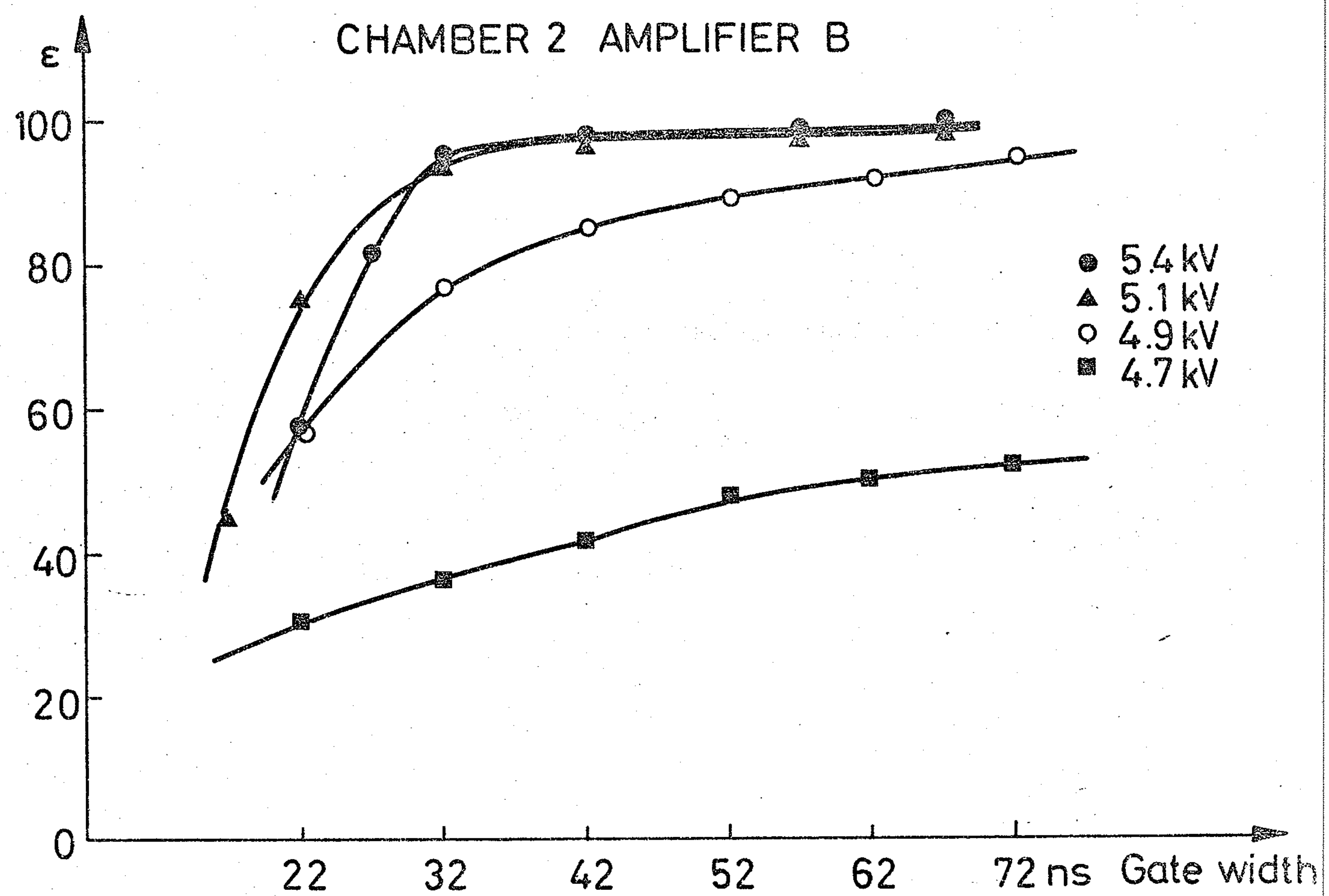
CHAMBER 2 AMPLIFIER B
ε
100
80
60
40
20
0
22
32
42
52
62
72 ns
Gate width
5.4 kV
5.1 kV
4.9 kV
4.7 kV

FIG. 19